

Spatial and Temporal Stochastic Interaction in Neuronal Assemblies*

Thomas Wennekers and Nihat Ay

Max Planck Institute for Mathematics in the Sciences
Inselstraße 22-26, D-04103 Leipzig, Germany

Abstract

The observation of various types of spatio-temporal correlations in spike patterns of multiple cortical neurons has shifted attention from rate coding paradigms to computational processes based on the precise timing of spikes in neuronal ensembles. In the present work we develop the notion of “spatial” and “temporal interaction” which provides measures for statistical dependences in coupled stochastic processes like multiple unit spike trains. We show that the classical Willshaw network and Abeles’ synfire chain model both reveal a moderate spatial interaction, but only the synfire chain model reveals a positive temporal interaction, too. Systems that maximize temporal interaction are shown to be almost deterministic globally, but possess almost unpredictable firing behavior on the single unit level.

Keywords: Spatio-temporal spike patterns; Gamma-oscillations; Synfire chains; Information geometry; Temporal Information maximization;

1 Introduction

It is a common belief that higher brain functions are expressed in coordinated activity of a vast number of neurons distributed throughout cortical

*Theory in Biosciences 122 (2003) 5–18.

and subcortical structures, that become integrated into functional networks on the large scale. The concept of “cell assemblies” proposed by Donald Hebb (1949) can be seen an early formulation of this idea with reference to neuronal representations of objects and more abstract entities in our subjective experience. According to Hebb, discrete entities are represented by distributed ensembles of cells that are mutually connected by strong and/or numerous synapses. Activation of part of an assembly thereby enables retrieval or “ignition” of the rest of the assembly, interpretable as a simple form of an “association”. The strong connections further support short-term memory in an assembly in form of persistent activity after the primary activating stimulus is withdrawn. Hebb’s assembly concept thus suggests explicit relations between anatomical connectivity, physiological firing activity, and psychological phenomena concerning object recognition and memory.

Evidence for short-term memory in form of persistent activity has indeed been given (cf., Fuster 1994) and experiments have also demonstrated synaptic plasticity in neural circuits (e.g., Bliss and Collingridge 1993; and many more), which could provide a correlation based learning mechanism for assembly formation as already required by Hebb. A direct empirical validation of the cell assembly hypothesis, however, is difficult. Correlation studies on real data demonstrated that stochastic interactions do not only take place on the level of firing rates: Beyond a simple coactivation of cells, as sufficient for Hebb’s basic hypothesis, there is increasing evidence that the precise relative timing of neuronal firing events actively takes part in computational processes. These observations have shifted the focus of attention from the rate coding paradigm to spike based concepts.

In the present work we briefly review the two types of spike-correlations that have reach most attention so far: Synchronized oscillations (reviews in Singer and Gray 1995; Eckhorn 1995) and repetitive “synfire patterns” (Abeles 1991). We show how theses patterns can in principle be explained in simple associative network models, but also demonstrate that there is in general no obvious and unique relation between the physical (synaptic) connectivity in a network and so-called “functional couplings” expressed by correlations in the observable spike trains (Aertsen et al. 1989). Physical and functional couplings are, therefore, at least in part independent. Targeting on a theory of statistical dependences we then formulate measures of “spatial” and “temporal stochastic interaction” without reference to any network models but only to statistical properties of spike trains. The mathematical framework has an intuitive interpretation in terms of information geometry,

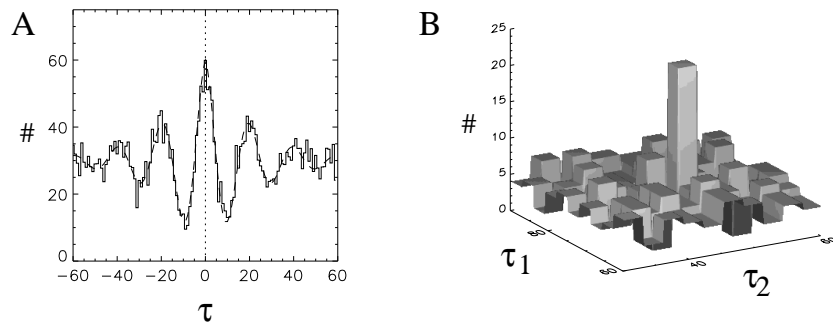


Figure 1: Correlation patterns in spike-trains. Left: Synchronized oscillation of 2 neurons; Right: Synfire pattern comprising 3 units, i.e., 2 time-shifts.

worked out by Amari (2001) for spatial interaction. We compare spatial and temporal interaction for simple associative networks, and consider systems with maximized temporal interaction. A formal characterization of stochastic interactions should provide a framework to understand also the relation between physical networks and observable spike trains more precisely.

2 Spike-correlations and Associative Models

Simultaneous recordings of several cortical units at once revealed various types of correlation patterns on the time-scale of single spikes. The left plot in Fig. 1, for example, displays the correlation function of two (artificially generated) spike trains and reveals a dominant peak at time zero indicative for frequent synchronous firings. In contrast, the smaller side-peaks at $\pm 20, 40, \dots$ milliseconds relate to a preference of the cells to fire periodically (here at 50Hz in the gamma-range), although jitter abolishes any covariation for τ larger than perhaps 80 or 100ms. “Synchronized gamma-oscillations” of this type in real data have been proposed as expressing the binding of feature coding neurons into “coherent” object representations (Singer and Gray 1995, Eckhorn 1999). The right plot in Fig. 1 displays part of a correlation function for three units (again using artificially generated data). The abscissa counts the number of occurrences of spike-patterns in a long trial, where the first unit fires at some time t , the second unit fires τ_1 ms later, and the third one τ_2 ms after the first. Most triplets defined by τ_1 and τ_2 occur at a low rate consistent with the assumption of independent firing.

The prominent peak in Fig. 1 (right), however, defines a certain pattern that appears significantly more often than chance level. Recordings from monkey prefrontal cortex by Abeles (1991) indicate that such “synfire patterns” occur in a behavior-dependent manner, but their functional role still is unknown.

Attempts have been made, to relate the above types of spatio-temporal correlations to tentative network architectures. These networks are instances of associative memories. The classical Hebbian ideas, for instance, can be formalized by the Willshaw auto-associative memory (Willshaw et al. 1969; Palm 1982; Amit 1995), which comprises a number of binary threshold units and stores a set of random patterns in the synaptic matrix between the cells by strengthening the synapses connecting active units in each pattern (the correlation learning rule or Hebb-rule). Patterns in an auto-associative Willshaw net correspond with assemblies in the Hebbian sense: The network reveals pattern completion in response to noisy or partial input patterns (association and ignition) as well as persistent activity (short term memory). However, it does not reveal complicated types of correlated activity. Once activated, cells in a pattern “fire” (that is, output a 1) in every time-step.

Using slightly more detailed single units or coupling schemes in associative networks easily introduces more complex correlations. Figure 2 displays simulations where the cells are so-called leaky-integrate-and-fire neurons (e.g., Dayan and Abbott 2001). Those represent the membrane potential of real neurons by a continuous internal variable, fire a spike if the potential exceeds a certain fixed threshold, but are reset to a resting potential afterwards to mimic after-hyperpolarization and avoid immediate further firings for some “refractory” time. Single spikes evoke post-synaptic potential changes on connected target neurons which smoothly increase up to some maximum value and decay afterwards in accordance with the form of unitary post-synaptic potentials (PSPs) in real neurons. Figure 2A shows an (auto-)associative synaptic coupling matrix storing six non-overlapping patterns in a network of 36 units as it could also appear in the simple Willshaw net. Figures 2B and C reveal two possible modes of persistent dynamic activity in the net as raster plots over time: Each dot in the figure represents the firing of a cell at the respective time. As can be seen in B all neurons of the first pattern fire periodically and synchronized. Although more detailed models for synchronized gamma-oscillations have been proposed, the example shown here is the most simple one that explains prototypically the type of correlations in Fig. 1A. Nonetheless, as Fig. 2C displays, where the fifth pattern has been excited, the same model reveals a second mode of behav-

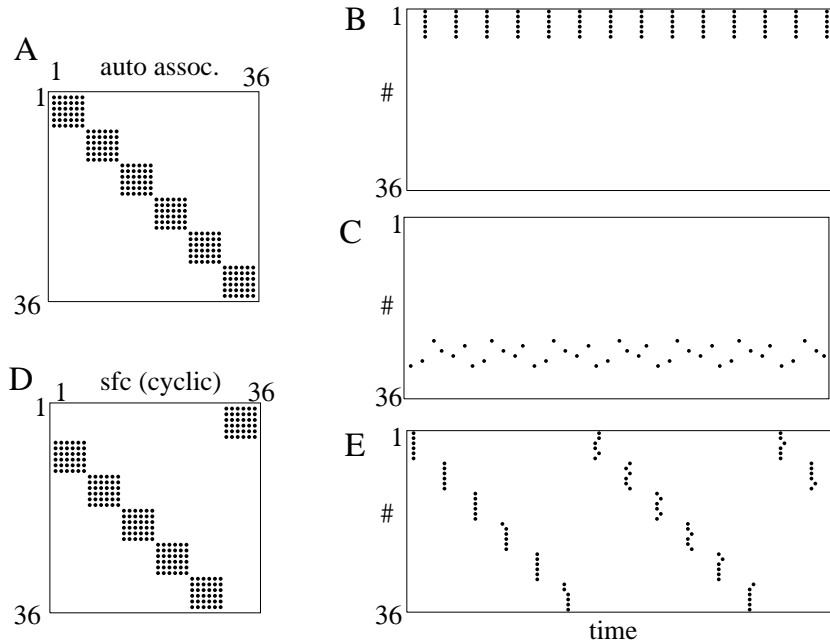


Figure 2: A: Auto-associative synaptic coupling matrix storing six non-overlapping patterns of six neurons each. B and C: Persistent synchronized (B) and asynchronous (C) activity as a raster plot over time in a network of spiking neurons. D: Hetero-associative cycle of six patterns (synfire chain model). E: Ordered retrieval of the stored sequence.

ior, where neurons still fire periodically, but asynchronously. Moreover, both modes of behavior can still be observed if the model is diluted, e.g., if a fraction of randomly selected synapses is set unfunctional, thereby changing the network connectivity. Thus, the type of spike patterns and correlations observable in simulations is not a unique function of the network connectivity; it depends in an intricate way on other constraints, too.

Fig. 2D shows a connectivity matrix, where six patterns have been stored in cyclic order: Neurons in each pattern project exclusively onto cells in the next pattern, a special case of “hetero-association”. Correspondingly, the model dynamics consists in a sequence of firings of the whole patterns, see Fig. 2E. This model is basically the “synfire chain model” as proposed by Abeles (1991) in order to explain precise repeating firing patterns as described in Fig. 1B. However, observe that also the active cells in Fig. 2C fire

in a fixed temporal order although they are homogeneously coupled. Thus, repeating firing patterns can in principle occur in different architectures.

These simple examples show two things: 1) The same architecture can in general lead to various types of firing patterns, and 2) different architectures can lead to spike patterns with comparable properties. It is, thus, usually impossible to infer unique physical connectivity structures from correlation patterns in spatio-temporal activity, the only data available from multiple unit recordings. Clearly, the situation in real neural systems is much more complex than our examples, but this makes the problem even more severe (Aertsen et al. 1989; Martignon et al. 1995). Therefore, one should carefully distinguish between the correlation structure in spike data and the underlying physical connectivity. Hebb’s suggestion that both are closely related, although to some degree intuitive, is anything but obvious in the light of real data. Accordingly, signatures of cell assemblies in observed data are a matter of interpretation, the more since even in the simplest models the relation between connectivity and the possibly observable firing patterns is intricate.

In the following we focus on the principal nature of stochastic interactions in spatio-temporal data without reference to network models. We try to formalize concepts for “stochastic interaction” as a starting point for a mathematical description of correlations and interactions in neural activity.

3 Spatial Stochastic Interaction

In order to illustrate the basic geometric idea behind spatial stochastic interaction, we consider an example system that consists of two units with binary state sets $\Omega_1 = \Omega_2 = \{0, 1\}$. The configuration set of the whole system is just the product $\Omega := \Omega_1 \times \Omega_2 = \{0, 1\} \times \{0, 1\} = \{(0, 0), (1, 0), (0, 1), (1, 1)\}$. We further assume that the occurrence probabilities of these configurations are given by a distribution p on Ω . Because the probabilities sum up to 1, the set of all probability distributions on Ω forms a three-dimensional simplex \mathcal{P}_2 with extremal points equivalent to Dirac measures concentrated in the individual configurations, see Fig. 3. The two units are considered independent with respect to a given distribution p if p can be factorized as

$$p(\omega_1, \omega_2) = p_1(\omega_1) p_2(\omega_2), \quad \omega_1, \omega_2 \in \{0, 1\} . \quad (1)$$

We denote the set of distributions that can be factorized by \mathcal{F}_2 . The set \mathcal{F}_2 forms a two-dimensional family of distributions (with boundary) in \mathcal{P}_2 , a so-

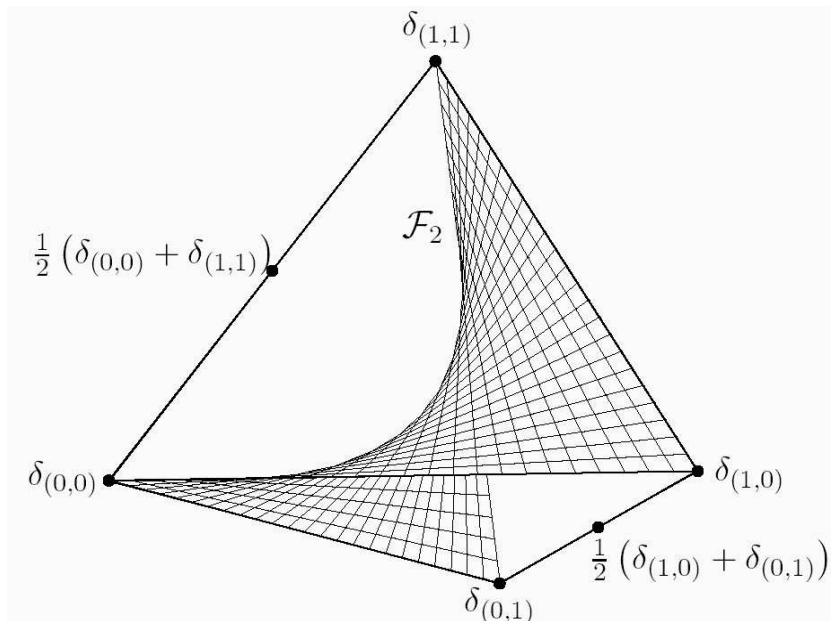


Figure 3: Simplex of probability distributions for two binary units and embedded “exponential family”, \mathcal{F}_2 , comprising independent distributions. “Spatial stochastic interaction” measures the (shortest) distance of a distribution from \mathcal{F}_2 and, therefore, quantifies stochastic dependence.

called “exponential family”. Now observe, that the distance of any particular distribution p from the set of factorized distributions \mathcal{F}_2 can be considered as a measure for spatial stochastic interaction, thereby providing an intuitive picture relating stochastic dependences and geometry in the simplex of probability distributions, \mathcal{P}_2 . Using the Kullback-Leibler (KL) divergence to quantify the “distance” of probability distributions (see Cover and Thomas 1991), we get as a measure for spatial stochastic interaction

$$D(p \parallel \mathcal{F}_2) := \inf_{q \in \mathcal{F}_2} D(p \parallel q) = H(p_1) + H(p_2) - H(p). \quad (2)$$

This is the well-known mutual information or transinformation of the two units with respect to p expressed in terms of Shannon-entropies.

It is straightforward to extend the previous example to N binary units $1, 2, \dots, N$, such that the configuration set is given by $\{0, 1\}^N$. In that case,

the set \mathcal{P}_N of probability distributions on $\{0, 1\}^N$ is still a simplex, but now of dimension $2^N - 1$. In contrast to this exponential growth of $\dim \mathcal{P}_N$, the dimension of the set \mathcal{F}_N of factorizable distributions grows only linearly in N : $\dim \mathcal{F}_N = N$. As before we consider the KL-distance of a distribution $p \in \mathcal{P}_N$ from the set \mathcal{F}_N as a measure for spatial stochastic interaction:

$$I(p) := D(p \parallel \mathcal{F}_N) = \inf_{q \in \mathcal{F}_N} D(p \parallel q) = \sum_{v=1}^N H(p_v) - H(p). \quad (3)$$

Amari (2001) discussed this measure for spatial stochastic interaction from the information-geometric point of view. Ay (2002a) studied probability distributions that maximize I . Tononi et al. (1994) used $I(p)$ (termed “integration” in their work) to quantify functional segregation in cortex.

4 Temporal Stochastic Interaction

Spatial stochastic interaction refers solely to probability distributions on the configuration space and ignores temporal structure inherent in state-transitions. Thus, a notion of temporal interaction seems necessary to approach the intrinsically temporal information contained in neural spike trains. Therefore, we extend the geometric concept of interaction from the spatial setting to the temporal domain. As a suitable tool we use Markov kernels to describe the transitions of the system states in time. A Markov kernel is a map $K : \{0, 1\}^N \times \{0, 1\}^N \rightarrow [0, 1]$, $(\omega, \omega') \mapsto K(\omega' | \omega)$, that gives the probability to be in configuration ω' in the next time step if the system is currently in ω . With \mathcal{K}_N we denote the set of all transition kernels K . The distance between two kernels K and L with respect to a probability distribution $p \in \mathcal{P}_N$ can be measured by a generalized version of the KL-distance:

$$D_p(K \parallel L) := \sum_{\omega, \omega' \in \{0, 1\}^N} p(\omega) K(\omega' | \omega) \ln \frac{K(\omega' | \omega)}{L(\omega' | \omega)}. \quad (4)$$

In order to quantify temporal stochastic interaction with respect to a kernel $K \in \mathcal{K}_N$, we need an analogue to the set \mathcal{F}_N of factorized distributions in the purely spatial setting. This is given by split Markov kernels. A kernel $K \in \mathcal{K}_N$ is called *split* if there exist kernels $K_1, \dots, K_N \in \mathcal{K}_1$ with

$$K(\omega'_1, \dots, \omega'_N | \omega_1, \dots, \omega_N) = K_1(\omega'_1 | \omega_1) \cdots K_N(\omega'_N | \omega_N).$$

The set of split kernels is denoted by \mathcal{K}_{spl} . We then define temporal stochastic interaction of the units with respect to the transition kernel K and a probability distribution p as the distance of K from the set of split kernels:

$$I(p, K) := \inf_{L \in \mathcal{K}_{spl}} D_p(K \| L) .$$

In order to derive a representation in terms of entropies analogous to (3) we define the conditional entropy of a transition (p, K) as

$$H(p, K) := - \sum_{\omega, \omega' \in \{0,1\}^N} p(\omega) K(\omega' | \omega) \ln K(\omega' | \omega) ,$$

and the marginal kernels as

$$K_v(\omega'_v | \omega_v) := \frac{\sum_{\substack{\sigma, \sigma' \in \{0,1\}^N \\ \sigma_v = \omega_v, \sigma'_v = \omega'_v}} p(\sigma) K(\sigma' | \sigma)}{\sum_{\substack{\sigma \in \{0,1\}^N \\ \sigma_v = \omega_v}} p(\sigma)} , \quad v = 1, \dots, N .$$

With these definitions, $I(p, K)$ has the following entropic representation:

$$I(p, K) = \sum_{v=1}^N H(p_v, K_v) - H(p, K) . \quad (5)$$

Formula (5) reduces to (3) for memoryless kernels, that is if $K(\omega' | \omega)$ does not depend on ω . Similar as $I(p)$, temporal interaction $I(p, K)$ can be interpreted in geometric terms as a distance from independence, but now for Markov transitions i.e., pairs (p, K) , and not just probability distributions. The measure for temporal stochastic interaction, $I(p, K)$, has been introduced in Ay (2003) and systems with interactions that maximize $I(p, K)$ have further been studied by Ay and Wennekers (2003), and Wennekers and Ay (2003).

5 Interaction in Simple Associative Systems

We come back to the spike timing patterns in Fig. 1, more precisely, their tentative explanation in terms of associative networks. To keep the following example as simple as possible, we reduce the attractor network and synfire chain dynamics to their most basic form: That is, we assume non-overlapping patterns, neglect noise, and assume that the single cells are just threshold units instead of integrate and fire cells. In that case, the cells in an excited

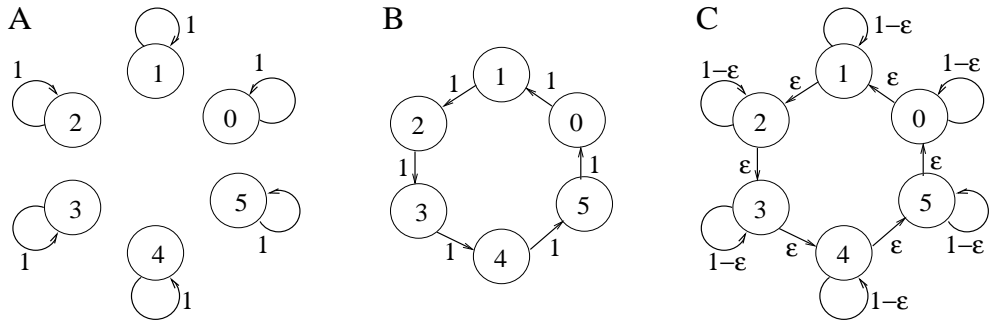


Figure 4: Transition diagrams for (A) the auto-associative and (B) the synfire chain model and six stored patterns. Labels at edges denote one-step transition probabilities. The graph in (C) contains (A) and (B) as limiting cases for $\epsilon = 0$ and 1, respectively.

assembly in the auto-associative memory fire in every step (so, there are no longer different synchronous and asynchronous modes as in Fig. 2B and C), and in the synfire chain model successive patterns fire at a delay of one simulated time-step, cf., Fig. 2E. Figure 4 depicts the situation schematically for six stored patterns. Intuitively, in the attractor model there is no temporal interaction because the firing pattern is constant, but in the synfire chain model we have a cyclic pattern sequence which corresponds to a certain information flow and a positive temporal stochastic interaction. We give formulas for $I(p, K)$ below in accordance with that intuitive reasoning.

Formally, we consider M patterns $s^i = (s_1^i, \dots, s_N^i) \in \{0, 1\}^N$, $i = 0, 1, \dots, M - 1$ such that for all units $v \in \{1, \dots, N\}$: $|\{i : s_v^i = 1\}| \leq 1$ (that is, each unit is in at most one pattern). We define the (support) size of the patterns s^i as $N_i := |\{v : s_v^i = 1\}|$, and their average size as $\bar{N} := \frac{1}{M} \sum_{i=0}^{M-1} N_i$. We further use a parametric family of transition kernels, corresponding with Fig. 4C, with the property

$$K^\epsilon(s^i | s^j) := \begin{cases} \epsilon & , \text{ if } i = (j + 1) \bmod M \\ 1 - \epsilon & , \text{ if } i = j \\ 0 & , \text{ otherwise} \end{cases} \quad , \quad \epsilon \in [0, 1] .$$

The probability distribution $p := \frac{1}{M} \sum_{i=0}^{M-1} \delta_{s^i}$ is stationary for all tran-

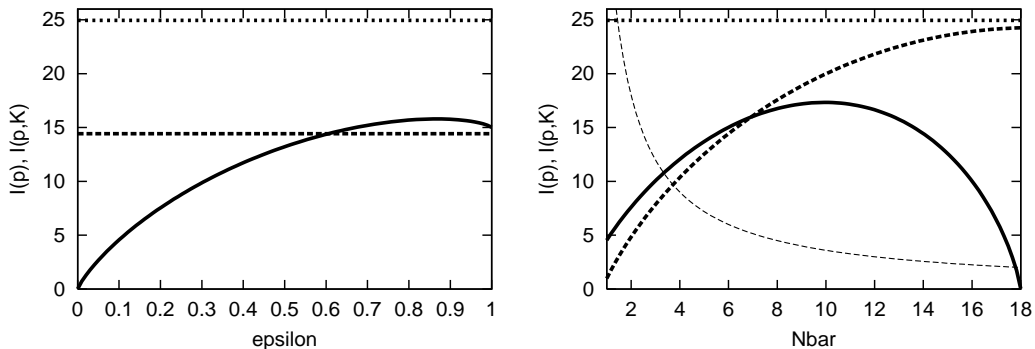


Figure 5: Temporal (solid) and spatial interaction (dashed) in the Willshaw associative memory; dotted line: maximally possible value, $N \ln 2 \approx 24.95$. Left: Interaction as function of ε with $N = 36$, $\bar{N} = 6$, $M = 6$. Right: Interaction as a function of pattern size \bar{N} with $N = 36$, $M = N/\bar{N}$, $\varepsilon = 1$. The thin line represents the number of storable (non-overlapping) patterns.

sition kernels K^ε . With these definitions, $I(p)$ results from (3) as

$$\begin{aligned} I(p) &= \left(\sum_{i=0}^{M-1} N_i \right) \cdot \left(-\frac{1}{M} \ln \frac{1}{M} - \frac{M-1}{M} \ln \frac{M-1}{M} \right) - \ln M \\ &= (\bar{N}M - 1) \ln M - \bar{N}(M-1) \ln(M-1), \end{aligned}$$

which obviously is independent of ε . Now, we compute the temporal stochastic interaction. The marginal kernels K_v^ε are for all v

$$K_v^\varepsilon(0|0) = \frac{M-1-\varepsilon}{M-1}, \quad K_v^\varepsilon(1|0) = \frac{\varepsilon}{M-1}, \quad K_v^\varepsilon(0|1) = \varepsilon, \quad K_v^\varepsilon(1|1) = 1-\varepsilon.$$

Using these kernels and the entropic representation (5), it is straightforward to derive the following expression for the temporal stochastic interaction:

$$\begin{aligned} I(p, K^\varepsilon) &= \bar{N}(M-1) \ln(M-1) - \bar{N}(M-1-\varepsilon) \ln(M-1-\varepsilon) \\ &\quad - (2\bar{N}-1) \varepsilon \ln \varepsilon - (\bar{N}-1)(1-\varepsilon) \ln(1-\varepsilon). \end{aligned}$$

Figure 5 (left) displays $I(p)$ and $I(p, K)$ for $M = 6$ and $N_i = \bar{N} = 6$, $i = 0, \dots, 5$ as in Fig. 2A and D. Apparently, $I(p) = 14.4$ is constant at roughly 58 percent of the maximally possible value of $36 \ln 2 = 24.95$ for 36 independent binary units. So, the attractor and synfire chain dynamics have equal spatial

interaction. Nonetheless, as Fig. 5 (left) shows, the attractor dynamics ($\epsilon = 0$) has zero temporal interaction, whereas that of the synfire dynamics ($\epsilon = 1$) is positive. Figure 5 (right) displays interaction values as a function of pattern size for $\epsilon = 1$, i.e., the synfire chain model. Increasing pattern size decreases the number of storable (non-overlapping) patterns (thin line). For $\bar{N} = N/2 = 18$ we can store just two patterns which must therefore alternate in each step ($\epsilon = 1$). Accordingly, the temporal interaction becomes zero, because the single unit dynamics are just bit reversals and, whence, perfectly predictable. Conversely, for $\bar{N} = 1$, units are silent for $N - 1$ steps after firing and, thus, again almost predictable corresponding with a low interaction. Only for intermediate pattern sizes the temporal interaction can be large. In contrast, spatial interaction increases monotonically and obtains its optimal value at $\bar{N} = N/2 = 18$, where $M = 2$ such that the single unit entropies are maximal (each unit is 0 in one pattern and 1 in the other). These entropies decrease for smaller patterns such that $I(p)$ gets small for small \bar{N} . The picture remains basically the same for larger networks, but note, that storage of a reasonable number of patterns requires small pattern sizes. Then the interaction values may fall considerably below the maximum value of $N \ln 2$. As we will show elsewhere, *overlapping* patterns, e.g., random patterns, in that regime again result in interactions that reach a moderately high fraction of the maximally possible values.

6 Strong Interaction and Determinism

In the previous section we found that stochastic interaction in “classical” associative models can have moderately high values. Some authors indeed argued that neurons maximize the information in their outputs about stimuli presented as inputs (Linsker 1986; Rieke et al. 1998; Dayan and Abbott 2001). Linsker’s Infomax principle, for instance, is related to the maximization of spatial interaction in feedforward neural networks (Ay 2002b). We therefore explored a generalized “Temporal Infomax Principle” that maximizes temporal interaction in recurrent systems (Ay and Wennekers 2003). The present section summarizes the results. For that purpose, Fig. 6 displays a simple example of a Markov chain comprising three units with numerically optimized temporal interaction: Starting from a random Markov kernel, K , that kernel was iteratively perturbed such that the temporal interaction increased to high values (cf. Ay and Wennekers 2003 for details). Interestingly,

activation patterns, after transients have died out, reveal deterministic configuration sequences of various lengths concatenated in an apparently random fashion. This is clearly visible in Fig. 6 (bottom), but in larger systems the deterministic subsequences easily become long and complex, and hardly distinguishable from independent random patterns by visual inspection only (examples can be found in (Ay and Wennekers 2003)).

7 Conclusions

In summary, we argued that the classical concept of Hebbian cell assemblies states a close relation between the physical connectivity in an assembly, functional couplings, i.e., covariations in physiological activation patterns, and psychological memory contents. These ideas can be well formalized in auto-associative Willshaw networks. However, in search for signatures of assemblies in real data, the correlation structure in multiple unit recordings turned out to be considerably complex. The observation of various patterns of oscillatory and synchronized behavior, repeating spike patterns, and fast modulations of functional connectivities indeed shifted the experimental focus towards cortical processing on the level of spikes and their relative timing. In parallel, associative network models already with slightly more realistic spiking neurons than the classical Willshaw net explained some of the observed phenomena, but they also demonstrated a non-unique relation between network anatomy and functional connectivities. These experimental and computational observations render a simple relation between connectivity and spike correlations in cortical networks questionable. Possible links are only partially available to date, mainly from computational network studies that addressed correlation patterns like synchronized oscillations and synfire patterns using different network schemes and single unit types.

In order to characterize functional couplings, we developed measures for spatial and temporal stochastic dependences on the base of statistical properties of observable multiple unit activity, i.e., occurrence probabilities for spike configurations and transition kernels. These measures provide an intuitive interpretation in terms of information geometry and may eventually result in a comprehensive mathematical theory to explore the structure of stochastic dependences in multiple unit data. The present paper, of course, only lays out the fundamental framework for such an approach, but related work seems promising (Amari 2001; Ay 2002ab; Nakahara and Amari 2002;

Wennekers and Ay 2003). A theory of stochastic interactions may further provide a base for advanced data analysis techniques (cf., e.g., Martignon et al. 1995; Grün et al 2002), and – in conjunction with network modeling as exemplified in section 5 – it may result in a deeper understanding how functional couplings can be related to network structures and their dynamics.

References

- [1] Abeles, M. (1991) *Corticonics: Neural circuits of the cerebral cortex*. Cambridge University Press, Cambridge UK.
- [2] Aertsen, A.M.H.J.; Gerstein, G.L.; Habib, M.K.; Palm, G. (1989) Dynamics of Neuronal Firing Correlation: Modulation of “Effective Connectivity”. *J.Neurophysiol.* 61:900–917.
- [3] Amari, S.-I. (2001) Information Geometry on Hierarchy of Probability Distributions. *IEEE Transactions on Information Theory* 47:1701–1711.
- [4] Amit, D.J. (1995) The Hebbian Paradigm Reintegrated: Local Reverberations as Internal Representations. *Beh. Brain Sci.* 18:617–657.
- [5] Ay, N. (2002a) An Information-Geometric Approach to a Theory of Pragmatic Structuring. *Annals of Probability* 30:416–436.
- [6] Ay, N. (2002b) Locality of Global Stochastic Interaction in Directed Acyclic Networks. *Neural Computation* 14:2959–2980.
- [7] Ay, N. (2003) Information Geometry on Complexity and Stochastic Interaction. *IEEE Trans. Inform. Theory*, submitted.
- [8] Ay, N.; Wennekers, T. (2003) Dynamical Properties of Strongly Interacting Markov Chains. *Neural Networks*, submitted.
- [9] Bliss, T.V.P.; Collingridge, G.L. (1993) A synaptic model of memory: long-term potentiation in the hippocampus. *Nature* 361:31–39.
- [10] Cover, T.M.; Thomas, J.A. (1991) *Elements of Information Theory*. Wiley Series in Telecommunications. New York: Wiley-Interscience.
- [11] Dayan, P.; Abbott, L.F. (2001) *Theoretical Neuroscience*. MIT-Press, Cambridge, MA.

- [12] Eckhorn, R. (1999) Neural mechanisms of scene segmentation: Recordings from the visual cortex suggest basic circuits for linking field models. *IEEE Transactions on Neural Networks* 10:464–479.
- [13] Fuster, J.M. (1994) *Memory in the cerebral cortex*. MIT Press, Cambridge.
- [14] Grün, S.; Diesmann, M.; Aertsen, A. (2002) Unitary events in multiple single-neuron spiking activity: I. Detection and significance. *Neural Comput.* 14:43-80. II. Nonstationary data. *Neural Comput.* 14:81-119.
- [15] Hebb, D.O. (1949) *The organization of behavior*. Wiley, New York.
- [16] Linsker, R. (1988) Self-organization in a perceptual network. *IEEE Computer* 21, 105–117.
- [17] Martignon, L.; von Hasseln, H.; Grün, S.; Aertsen, A.; Palm, G. (1995) Detecting higher-order interactions among the spiking events in a group of neurons. *Biol.Cybern.* 73:69–81.
- [18] Nakahara, H.; Amari, S. (2002) Information geometric measure for neural spike trains. *Neural Comput.* 14:2269–2316.
- [19] Palm, G. (1982) *Neural Assemblies. An Alternative Approach to Artificial Intelligence*, Springer Verlag, Berlin.
- [20] Rieke, F., Warland, D., Ruyter van Steveninck, R.; Bialek W. (1998) *Spikes: Exploring the Neural Code*. MIT Press, Cambridge.
- [21] Singer, W.; Gray, C.M. (1995) Visual feature integration and the temporal correlation hypotheses. *Ann.Rev.Neurosci.* 18:555-586.
- [22] Tononi, G.; Sporns, O.; Edelman, G.M. (1994) A measure for brain complexity: Relating functional segregation and integration in the nervous system. *Proc.Natl.Acad.Sci.* 91:5033–5037.
- [23] Wennekers, T.; Ay, N. (2002) Temporal Infomax on Markov Chains with Input Leads to Finite State Automata. *Neurocomputing*, in press.
- [24] Willshaw, D.J.; Buneman, O.P.; Longuet-Higgins, H.C. (1969) Non-holographic associative memory. *Nature* 222:960–962.